Nanotechnology and Precision Engineering 1 (2018) 180–186

Contents lists available at ScienceDirect

Nanotechnology and Precision Engineering

journal homepage: http://www.keaipublishing.com/en/journals/nanotechnology-and-precision-engineering/

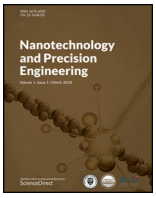

Kinematic error modeling and error compensation of desktop 3D printer

Shane Keaveney *, Pat Connolly, Eoin D. O'Cearbhaill

School of Mechanical and Materials Engineering, UCD Engineering and Materials Science Centre, Dublin 4, Ireland

ARTICLE INFO

Available online 17 October 2018

Keywords:
3D printing accuracy
Kinematic error modeling
Kinematic error compensation
Ballbar
FDM 3D printing
ISO230-4

ABSTRACT

Desktop 3D printers have revolutionized how designers and makers prototype and manufacture certain products. Highly popular fuse deposition modeling (FDM) desktop printers have enabled a shift to low-cost consumer goods markets, through reduced capital equipment investment and consumable material costs. However, with this drive to reduce costs, the computer numerical control (CNC) systems implemented in FDM printers are often compromised by poor accuracy and contouring errors. This condition is most critical as users begin to use 3D-printed components in load-bearing applications or to perform mechanical functions. Improved methods of low-cost 3D printer calibration are needed before their open-design potential can be realized in applications, including 3D-printed orthotics and prosthetics. This paper applies methodologies associated with high-precision CNC machining systems, namely, kinematic error modeling and compensation coupled with standardized test methods from ISO230-4, such as the ballbar for kinematic and dynamic error measurements, to examine the influence and feasibility for use on low-cost CNC/3D printing platforms. Recently, the U.S. Food and Drug Administration's "Technical considerations for additive manufactured medical devices" highlighted the need to develop standards specific to additive manufacturing in regulated manufacturing environments. This paper shows the benefits of the methods described within ISO230-4 for error assessment, alongside applying kinematic error modeling and compensation to the popular kinematic configuration of an Ultimaker 3D printer. A Renishaw ballbar QC10 is used to quantify the Ultimaker's errors and thereby populate the error model. This method quantifies machine errors and populates these in a mathematical model of the CNC system. Then, a post-processor can be used to compensate the printing code. Subsequently, the ballbar is used to demonstrate the dramatic impact of the error compensation model on the accuracy and contouring of the Ultimaker printer with 58% reduction in overall circularity error and 90% reduction in squareness error.

1. Introduction

Current developments in the 3D printing industry have revolutionized the way people consider the manufacturing process. 3D printing has provided open access to critical aspects of the product design cycle including materials, design, prototyping, and manufacturing avenues. The prototyping and manufacturing stages of design have been brought closer to innovators from both technical and non-technical backgrounds. 3D printing offers design and material freedom, speed of development, and reduced capital investment in manufacturing.[1] The rewards of these key advantages have been observed in medicine and medical devices together with assistive technology due to the capability to produce user-specific and advanced material constructs and scaffolds.

Many 3D printing technologies rely on computer numerical control (CNC) systems for precise and accurate processing. Given the nature of additive manufacturing, precision and accuracy are critical to the fundamental layering mechanism. Any fault or misalignment in this process can have a dramatic effect on the component's performance. Moreover, errors are magnified with the emerging trend of multi-axis processing in additive manufacturing,[2] as observed previously in subtractive manufacturing. The accuracy and precision of the multi-axis CNC system is largely influenced by control and mechanical errors that directly affect the relative position between the print head and workpiece.

This study is based on two motivations: one is the application of methods used for precision CNC subtractive manufacturing[3] to additive and the other is the application of methods used in ISO standards for error assessment. Other methods of error compensation for 3D printing began to emerge,[4] but this study uses the ballbar method in ISO 230-4[5] for error assessment, with kinematic error modeling[6] for compensation of the axes errors. The FDA recently released a technical document on additive manufactured medical devices.[7] This paper aims to build a basic model of error compensation and assessment that can inform future standards in regulated manufacturing, including that of medical devices.

A major concern in advanced subtractive manufacturing processes is the variation of direction and quantity of cutting forces, which requires highly stiff machine tools to avoid inaccuracy and vibrations.[8] In high-precision CNC systems with ballscrew feed systems, achieving micron

* Corresponding author.
E-mail address: shane.keaveney@ucd.ie (S. Keaveney).

https://doi.org/10.1016/j.npe.2018.09.002

accuracy is challenging.[9,10] This condition limits the use of multi-axis robots for high-precision subtractive manufacturing. Due to the low mechanical loads in typical 3D printing processes, machine stiffness is not as important, making these processes suitable for multi-axis manufacturing. While recognizing gravitational effects, this can provide print-head orientation freedom and extreme access capabilities. Before moving on to more complex multi-axis systems, we have to understand and quantify errors in simplistic *XYZ*-axis additive systems.

This paper demonstrates the capabilities of kinematic error modeling and compensation for a low-cost basic 3D printer called Ultimaker Original. This task is achieved through pre-compensation of the part program to run the printer. The methodologies applied here can be translated to multi-axis 3D printers in future studies. The Ultimaker Original is chosen as a demonstrator because it is affordable and has parallel kinematic configuration. A Renishaw QC10 Ballbar with resolution of 0.1 μm is used to quantify the printer's errors before and after compensation.

2. Materials and methods

A kinematic error model was developed for the Ultimaker Original 3D printer with a G-code post-processor used to perform pre-compensation. The kinematic configuration of an Ultimaker is not a typical serial kinematic configuration; hence, a unique model is required, i.e., the axes are theoretically independent, whereas in a serial kinematic configuration, the order of axis assembly directly affects the influence of each axis on the subsequent axis on the chain.

2.1. 3D printer kinematic error assessment

Kinematic errors, which are geometrical, include axis alignment, straightness, yaw, and pitch-and-roll errors.[11] The ballbar introduced in the mid-1980s[12] is a popular and effective method of machine calibration under no-load conditions, enabling kinematic and dynamic error identification and quantification.[11] A Renishaw QC10 ballbar with Renishaw "Ballbar 20" software was used for this study, as shown in Fig. 1. The ballbar itself is a double-acting linear variable differential transformer (LVDT) with a resolution of 0.1 μm. The ballbar measures variation from a nominal radial distance between two points programmed to move in relative circular motion on the CNC machine. The Ballbar 20 software uses time and feedrate/speed to infer angular position. This method provides a polar coordinate to track the end effector to a resolution determined by the sampling rate of approximately 25 Hz. Tests are conducted in both feed directions, thereby enabling analysis of the results and estimation of axes errors.

The simplicity of the ballbar device through its single measurement element and error-free magnetic joints allows for a quick assessment of the machine accuracy with minimal setup time and high repeatability. Extensive research has been conducted using the ballbar for translational and rotational axes error assessment extending to inferences for multi-axis contouring performance.[13] One of the major criticisms on the ballbar method is the reliance on time to record the angular positioning of the tool centerpoint (TCP) at a given sample point. This issue has been addressed by using a radial encoder for angular tracking, but this additional encoder increases the setup complexity.[14]

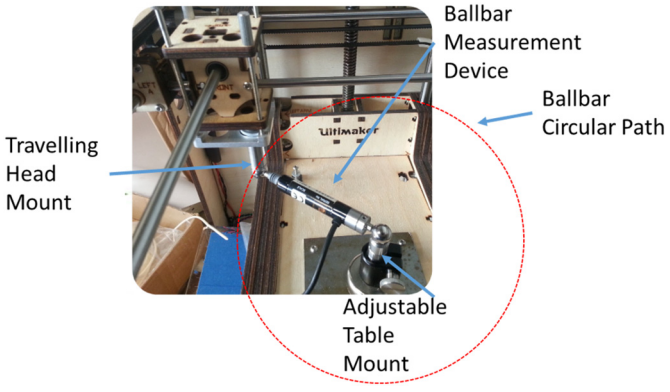

Fig. 1. Ballbar setup on Ultimaker Original with modifications to printer.

2.2. Experimental setup

The experimental program set out to investigate the geometric errors of the Ultimaker Original 3D printer and the response of the system to compensation for detected errors modeled to include squareness, scale, and backlash. The influence of feedrate was investigated deeply, but preliminary results are shown for its influence. A default feedrate of 1850 mm/min was used as a representative of what would be used for printing and fits with ISO 230-4, with tests taken in both feed directions. A nominal ballbar radius of 100 mm was used. Printer modifications were required for ballbar mounting. The ballbar needs two reference/mounting points on the machine. Typically, these are a machine tool table and tool holder. As the printer does not have a tool holder and the bed is nonferrous, an improvised tool head and metal table were required, as shown in Fig. 1. For the results presented here, a series of ballbar tests were conducted, including a control and then a progressive incrementing of compensation factors. With this type of study, multiple refinements can be performed to tune the system to higher levels of accuracy, but this is not the goal of these experiments. The primary goal of the experimental section is to show that the method proposed is efficient and has a positive impact on the system accuracy. Owing to the construction of the printer, the focus was also on the *XY* accuracy because this is the most error-prone section of the printer. The methods used in the experimental plan can be easily applied to the *Z*-axis planes, but were not considered necessary in this proof-of-principle work. Both directions of travel were investigated, as is typical with ballbar testing, and the results across both directions are summarized.

The results of the subsequent ballbar tests were used to calculate the error values of the printer and thus to populate the kinematic error model. The error model was then implemented to compensate the ballbar part programs, i.e., a pre-compensation strategy. The error compensation was applied gradually to observe the effects on the system. Then, the ballbar test results were used to evaluate the error model's performance and the accuracy of the ballbar error predictions.

2.3. Kinematic error modeling

Kinematic machine errors are errors concerned with the kinematic structure of the machine. This model represents the errors of the kinematic chains that provide a representation of the effects of the errors on a given print path. These errors, which include axis alignment, axis straightness, yaw, pitch, roll, offset of center of rotation, and offset errors, can be predicted or measured directly through machine error assessment methods such as the ballbar used in this study. The kinematic error model is derived from previously established methods described by Srivastava et al.[15] These methods assume that each axis, rotational and translational, has six geometrical axis errors, as demonstrated in Fig. 2 (left). The alignment errors are between average axes lines of each axis. The theoretical average line through the axes relative to its movement over its range of motion is the axis average line.

The kinematic configuration developed for the Ultimaker 3D printer is shown in Fig. 2 (right). This is a parallel kinematic configuration, but it still has *X* and *Y* axes. Typically parallel kinematic configuration machines have no actual *XYZ* axes as shown in a DeltaWASP 3D printer configuration from WASP (CSP srl, Italy); the configuration is loosely based on Stewart platform principles.[16] The kinematic model treats the machine as a multi-body system consisting of a number of rigid bodies[17] spatially related to an adjacent body using 4×4 homogenous

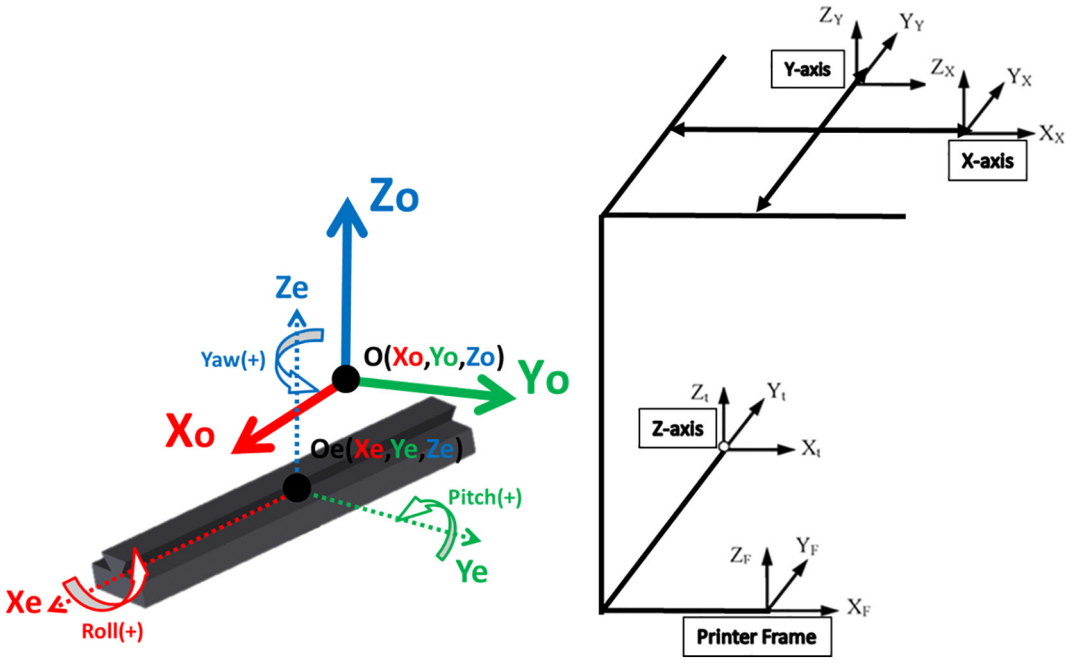

Fig. 2. (left) Visualisation of a translational axis: 6 kinematic errors, 3 translation, and 3 rotational; (right) kinematic configuration of Ultimaker Original showing the parallel chain configuration.

transformation matrices (HTMs) within the work coordinate system of the machine. These HTMs calculate the contribution of each axis error and relevant alignment error to the deviation of the actual nozzle position relative to the desired or commanded position. In certain cases, cancelation of errors can occur, whereby errors of one axis act against that of another, effectively reducing the effect on the overall error of a given toolpath. This interaction between axis errors causes difficulty in identifying individual axis errors and correcting the completion of error model variables. This condition would be even more complex with an increased number of axes such as in multi-axes robots, where singularities are much more likely to occur.

For the Ultimaker Original kinematic error model, an HTM is developed for each axis and for the axis alignment errors, which are described as H_X, H_Y, H_Z, and H_{AL} respectively. A sample HTM is provided for a pitch operation about the *Y*-axis and translational offset on an *X*-axis is shown in Eq. (1), where β is the pitch angle:

$$\mathrm{HTM} = \begin{bmatrix} \mathrm{Cos}(X_\beta) & 0 & \mathrm{sin}(X_\beta) & X_x \\ 0 & 1 & 0 & X_y \\ -\mathrm{Sin}(X_\beta) & 0 & \mathrm{cos}(X_\beta) & X_z \\ 0 & 0 & 0 & 1 \end{bmatrix}. \tag{1}$$

Considering the Ultimaker Original's configuration versus a serial CNC machine configuration, we find that in a serial configuration, the axis assembly order directly affects the error contribution of each axis. For example, if the *X*-axis sits on top of the *Y*-axis, then the errors of the *X*-axes will alter the *Y*-axes errors relative to the machine reference frame. In the case of the Ultimaker Original, the axes theoretically do not influence each other; thus, the contributions of each must be individually calculated. However, the orientation misalignments from each axis have a cumulative effect on the relative orientation of the nozzle to the workpiece. Based on the HTM in Eq. (1), the first three columns and rows are the orientation portion of the HTM, and the last column is the translation portion and scale factor set to 1 in this case. The first three columns of the bottom row can be ignored in this study. For this model, a desired point HTM is created, which allows for the calculation of the translation and orientation effect of each axis individually, as described in Eq. (2):

$$\mathrm{HTM}_{\mathrm{desired}} = \begin{bmatrix} 1 & 0 & 0 & X_{\mathrm{desired}} \\ 0 & 1 & 0 & Y_{\mathrm{desired}} \\ 0 & 0 & 1 & Z_{\mathrm{desired}} \\ 0 & 0 & 0 & 1 \end{bmatrix}. \tag{2}$$

To calculate the error contribution of each axis, the HTM in Eq. (2) is multiplied by the respective error HTMs for that axis, which is described in Eq. (3), where H_{ex} is the error HTM for the *X*-axis:

$$H_{ex} = H_X * \mathrm{HTM}_{\mathrm{desired}}. \tag{3}$$

From the resultant HTM, H_{ex} for the *X*-axis in this example, the contribution of the axis to the positional error is calculated by subtraction of the positional portion of H_{ex} by the desired positions represented in Eq. (2).

H_{ex}, H_{eY}, H_{eZ} can then be multiplied by each other to obtain H_{XYZerr} as follows:

$$H_{XYZerr} = H_{eY} * H_{ex} * H_{eZ}. \tag{4}$$

However, for H_{XYZerr}, the positional aspect of the HTM, i.e., the last column, has to be replaced with the sum contribution of each axis in relation to its contribution to the positional error. This task is performed by replacing the last column in H_{XYZerr} with the last column in $H_{\mathrm{Pcontribution}}$. Calculation of $H_{\mathrm{Pcontribution}}$ is described as follows:

$$H_{\mathrm{Pcontribution}} = (H_{\mathrm{eX}} - \mathrm{HTM}_{\mathrm{desired}}) + (H_{eY} - \mathrm{HTM}_{\mathrm{desired}}) + (H_{eZ} - \mathrm{HTM}_{\mathrm{desired}}). \tag{5}$$

Once H_{XYZerr} has been modified, it can be multiplied by H_{AL}, which describes the axis alignment errors as follows:

$$H_{\mathrm{total}} = H_{AL} * H_{XYZerr}. \tag{6}$$

H_{total} can then be used to determine the overall influence of the kinematic errors of the desired position. The desired position is considered

as a vector with a base point of (x_p, y_p, z_p) and an orientation described by the end point of a unit vector (x_o, y_o, z_o). This condition is described as P_{final}' according to Eq. (7):

$$P'_{final} = \begin{bmatrix} x_p \\ y_p \\ z_p \\ x_o \\ y_o \\ z_o \end{bmatrix}. \quad (7)$$

The base point is determined by multiplying a vector of the desired point by H_{total} as described by Eq. (8):

$$P'_{final-position} = H_{total}{}^{*} P_{desired}$$
$$\text{where } P_{desired} = \begin{bmatrix} X_{desired} \\ Y_{desired} \\ Z_{desired} \\ 1 \end{bmatrix} \text{ and } P_{final-position} = \begin{bmatrix} X_p \\ Y_p \\ Z_p \\ 1 \end{bmatrix} \quad (8)$$

The orientation is described by multiplying a unit vector aligned to the Z-axis by H_{total} as shown in Eq. (9):

$$P'_{final-orientation} = H_{total} * U_Z$$
$$\text{where } U_Z = \begin{bmatrix} 1 \\ 0 \\ 0 \\ 0 \end{bmatrix} \text{ and } P_{final-orientation} = \begin{bmatrix} X_o \\ Y_o \\ Z_o \\ 1 \end{bmatrix} \quad (9)$$

The values from $P_{final-position}$ and $P_{final-orientation}$ can be used to fill in P_{final}' respectively. In the Ultimaker Original printer error, compensation is only possible in the XYZ axis as no rotational axes are present. To determine the compensation, we calculate the difference between the desired and achieved positions by subtraction. The error can simply be added to the commanded position in the print program as the achieved position is that of the desired position.

The HTMs described earlier are representations of the axes errors, but the values used to populate these may vary throughout the working volume. Error quantification should be conducted in the correct volume of the machine to ensure accuracy of the model.

In this paper, backlash compensation was also applied. This is not described in the previous kinematic model because it is a dynamic error, which means that its influence is dependent on the movement of the machine. The algorithm used here scans the toolpath to detect backlash zones (i.e., areas where the axes change direction) and then applies a backlash compensation if required. There are two modes of backlash compensation: on and off. If backlash compensation is on, then a specific backlash offset is applied, i.e., backlash compensation is not only applied at the backlash zone but also along the toolpath until it is switched off.

3. Results

3.1. Ballbar testing: control

A control ballbar test was conducted on the Ultimaker Original 3D printer to record the errors of the machine using a Renishaw QC10 ballbar and associated software. From these experiments, control values for each of the critical errors were generated as shown in Table 1.

According to the results in Table 1, squareness error is the major contribution to circularity error. Squareness error is the angular discrepancy between the X and Y axes from 90°. This result is indicated as μm/meter rate, which means that if the machine traveled 1 m on the X-axis, the desired point would deviate by 3638.6 μm from the ideal toolpath in the Y direction. The X-axis is also shown to have a higher level of error contribution than the Y-axis. Under the independent circularity column, the effect of each error is observed in terms of circularity of the trace and its percentage contribution to the overall circularity error. This condition is highlighted for the focus errors in this study. Other errors are reported from the Ballbar 20 software, but this paper does not focus on them due to the complexity of compensation and their higher dependency on control (i.e., stepper motor resolution and belt-feed system) as opposed to kinematic errors that can be more easily compensated.

Table 1
Ballbar test results from test with no error compensation to measure the control or baseline level of kinematic and dynamic errors in X and Y axes.

Parameter	Value	Circularity contribution (μm)	Error contribution (%)
X-axis			
Backlash *X* (μm)	>4.4, <37.4	37.4	4
Reversal spikes *X* (μm)	>1.4, <-21.5	21.5	2
Lateral play *X* (μm)	>-60.2, <-123.8	96.9	11
Cyclic error *X* (μm)	>74.3, <107.9	97.2	11
Straightness *X* (μm/200 mm)	137	68.5	8
Scaling error *X* (ppm)	−451.7	–	–
Cyclic pitch *X* (mm)	31.75	–	–
Center offset *X* (μm)	123.8	–	–
Y-axis			
Backlash *Y* (μm)	^11.3, v5.4	11.3	1
Reversal spikes *Y* (μm)	^−9.6, v-3.5	9.6	1
Lateral play *Y* (μm)	^−45.2, v33.5	23.9	3
Cyclic error *Y* (μm)	^58.4, v30.6	51.9	6
Straightness *Y* (μm/200 mm)	−3.8	1.9	0
Scaling error *Y* (ppm)	287	–	–
Cyclic pitch *Y* (mm)	31.75	–	–
Centre offset *Y* (μm)	−68.2	–	–
XY axes combination			
Servo mismatch (ms)	0.62	19.6	2
Squareness (μm/m)	−3638.6	363.9	41
Scaling mismatch (ppm)	147.7	73.9	8
Positional tolerance (μm)	1541.1	–	–
Radius deviation (μm)	8.2	–	–
Feedrate programmed (mm/min)	1875	–	–
Feedrate calculated (mm/min)	1892.6	–	–
Circularity (Av.) (μm)	535.4	–	–
Circularity (CCW) (μm)	539.9	–	–
Circularity (CW) (μm)	456.1	–	–

Squareness error directly affects circularity; thus, an improvement in circularity is expected from the reduction of squareness error. Squareness and backlash errors are theoretically independent of the radius of the ballbar test; however, the circularity error is not. Some other errors of the machine's axes were examined, including axis straightness, but only a select number of common error contributors are compensated in this study to show the efficiency of the methodology applied. Fig. 3 shows the control trace in the counterclockwise (CCW) and clockwise (CW) directions of the ballbar test on the Ultimaker Original in the XY plane. The squareness error can be seen from the ovality of the trace, which is centered along an axis at 45° to X and the angle of the ovality to the X-axis is the same across both test directions. The red oval is overlaid onto the original ballbar trace to illustrate the identification of the squareness error. This condition is automatically performed by the Ballbar 20 software. Other errors can present themselves in a similar manner to squareness, but the angle of the center line of the oval trace changes with the travel direction between 45° and 135°, unlike the squareness error, which produces a 45° angle in both directions.

After the squareness error, backlash is the next major error identified. Backlash is the loss of feed drive between the stepper motor and the axis during a change of axis direction. Fig. 3 (bottom) shows an example of pure backlash on a simulated ballbar trace with no other errors. An important point that is critical for ultra-precision error compensation is the difference in backlash on either side of the circular trace. Table 1 shows that there are two values of backlash for each axis, i.e., X and Y. These values represent the backlash on either side of the axis direction change point on the circular trace, as shown in Fig. 3

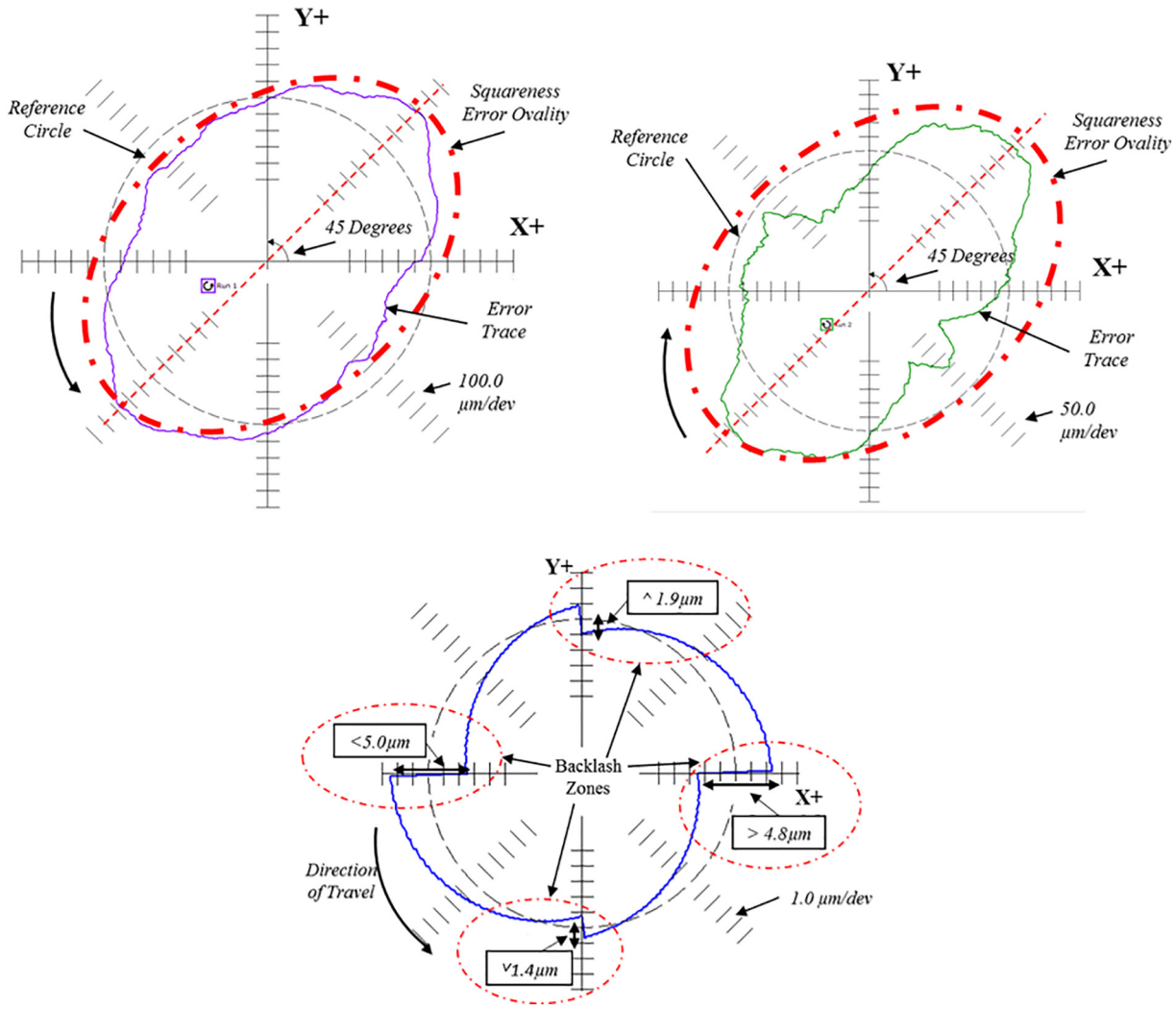

Fig. 3. (top left) Control ballbar result trace in CCW direction; (top right) control ballbar result trace in CW direction showing squareness error identification as no orientation change from CCW trace; (bottom) simulated pure backlash for demonstration of effect.

(bottom). The observed backlash looked similar to the reversal error, i.e., a loose motion error during change in the direction of an axis. This result is most likely due to the belt system use on the Ultimaker, which provides some slop during change of direction. One of the limitations of the backlash compensation method is that it is applied instantaneously as opposed to gradually over a defined range.

3.2. Ballbar testing: compensation

Following a thorough analysis of the results presented from the control Ballbar tests, the error model was applied to the ballbar toolpaths. Compensation of the squareness, scale, and backlash errors were applied sequentially to show their influence while also changing error values as these error compensations were coupled. The application of the compensation from the error models was easily implemented using the developed post-processor. The original ballbar programs were inputted into the G-code post-processor; the toolpaths processed and modified according to the model with a new print program outputted. These print programs were then used to perform the ballbar tests and the results were recorded using the Renishaw Ballbar 20 software, the same as for the control tests.

To apply the compensation factors, we introduced one error compensation initially and then others sequentially to prevent confounding of error compensation. Table 2 details the results achieved from the application of compensation combinations. The left side of the table shows the critical ballbar results and the corresponding result from the control tests. The compensation applied is shown at the bottom of the table. Compensation of squareness error was performed using angular misalignment of axis, in degrees, to comply with the error model. The results in Table 2 show that applying the reported −3638.3 µm/mm of backlash reduced the squareness error to −78.3 µm/mm with a 36% decrease in circularity error. Applying scale error compensation in the *X* and *Y* axes brought the desired average trace radius from 99.9952 mm to 100.0001 mm, which means that the average radius was only 0.1 µm greater than programmed. However, scale compensation also influenced the squareness error, increasing its effect by 42.2 µm/mm.

To demonstrate the dynamics errors at play in the system, this test was repeated at a lower federate with the same squareness and scale error compensation applied. The result showed that the squareness error decreased, but the scale error in the *X*-axis increased with the desired radius of the ballbar trace decreasing by 4.2 µm.

Fig. 4 visually shows the improvements in contouring performance of this system through the kinematic error modeling and compensation applied. The 92% reduction in circularity effect from squareness from 363.9 µm to 27.7 µm has greatly improved contouring performance. Backlash compensation was finally applied to the *X* and *Y* axes with the *X*-axis responding somewhat positively and the *Y*-axis showing a

Table 2
Experimental results from application of error compensation using kinematic error model developed with measurement of error using the ballbar.

Parameter	Reported error value					
	Test 1	Test 2	Test 3	Test 4	Test 5	Test 6
Backlash *X* (μm)	>4.4, <37.4	>5.1, <65.9	>6.9, <61.9	>10.9, <77.8	>-64.2, <-3.5	>-64.6, <-9
Backlash *Y* (μm)	^11.3, v5.4	^32.8, v9.4	^44.1, v13.6	^61.1, v25	^47.6, v16.5	^47.7, v27.7
Squareness (μm/m)	−3638.6	−78.3	−120.5	−97.2	−127.5	276.9
Straightness *X* (μm/200 mm)	137	219.1	114.6	116.3	116	117.6
Straightness *Y* (μm/200 mm)	−3.8	−7.7	−10.3	−2.2	−6.1	−6.9
Scaling mismatch (ppm)	147.7	−40.8	−1.6	−13.6	3.1	7
Scaling error *X* (ppm)	−451.7	−150.2	−2.7	75.7	37.2	12.2
Scaling error *Y* (ppm)	287	53.9	5.2	−7.7	21.8	−22.8
Feedrate programmed (mm/min)	1875	1875	1875	625	1875	1875
Feedrate calculated (mm/min)	1892.6	1866.3	1868.1	624.4	1870	1866.3
Radius deviation (μm)	8.2	4.8	−0.1	4.2	−2.9	0.5
Circularity (Av.) (μm)	535.4	343.5	272.3	315.2	226.1	249.9
Circularity (CCW) (μm)	539.9	286.8	226.2	243.5	191.9	234.9
Circularity (CW) (μm)	456.1	324.6	257.8	300	238.5	232.2
Parameter	Compensation values					
	Test 1	Test 2	Test 3	Test 4	Test 5	Test 6
Backlash *X* (μm)	0	0	0	0	74.5	74.5
Backlash *Y* (μm)	0	0	0	0	0	42
XY squareness (deg)	0	−0.20847	−0.20847	−0.20847	−0.20847	−0.20847
Scale *X* (ppm)	0	0	−109	−109	−109	−109
Scale *Y* (ppm)	0	0	27.4	27.4	27.4	27.4

limited impact. The *X*-axis compensation shows that the application of a 74.5 μm compensation had an impact on the axis, with the right side backlash decreasing by 75 μm and the left side decreasing by 84 μm on average. These results illustrate the close relation between the change in backlash effect and backlash compensation level applied within 7%. For the *Y*-axis, the influence of the compensation is not directly related to the level of compensation applied in the model but is consistent. For the top of the *Y*-axis, we observe an approximately 14 μm reduction in backlash with only 0.1 μm in the bottom. This result shows that pure backlash is not the only factor that influences the accuracy of this axis in reversal errors.

4. Discussion

The objective of this study was to show the effectiveness of a simple kinematic error compensation model to improve the accuracy and precision of a low-cost, relatively imprecise CNC system used in 3D printing. In this case, repeat testing was not required due to the high accuracy of the ballbar, and 0.1 μm resolution relative to the printer's resolution, which was estimated at 200 μm in the *XY* axes. Moreover, this study did not aim to examine the repeatability of the 3D printer itself but the influence of the kinematic error model compensation. The findings show that when relative error compensation is applied, the desired result is observed from the ballbar test. This condition is particularly evident from the effect of applying squareness error compensation, where the squareness error compensation between tests 2 and 3 is applied with a reduction from a squareness error of −3638.6 μm/m to −78.3 μm/m. Similarly, scaling error compensation between tests 3 and 4 is applied with a reduction from 4.8 μm radial deviation to −0.1 μm. In the calibration of CNC machines, this is typically how error correction would be applied, varying single factors of compensation and repeating the ballbar test to ensure that the desired results are achieved. The proposed kinematic error model and the compensation methods can be applied and adopted for other systems. The model is easily reconfigured for systems that have Cartesian linear axes configurations, as is the case for most CNC systems outside the steward platform-style systems previously discussed.

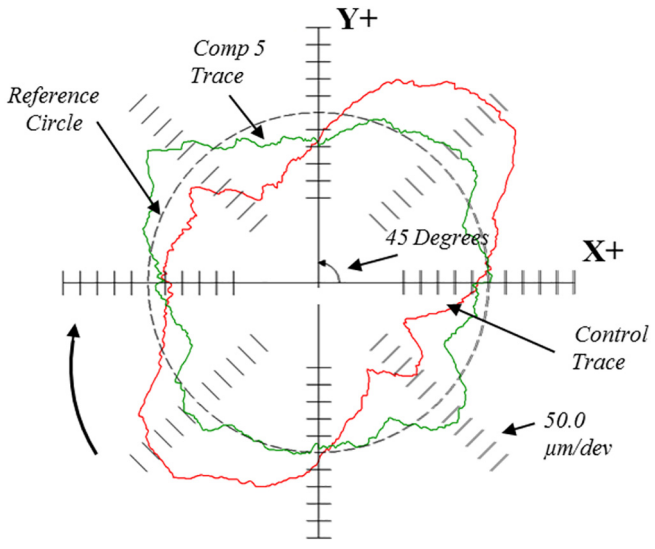

Fig. 4. Comparison of uncompensated ballbar test trace (red) versus compensated ballbar test trace (green) showing the improvement in contouring and accuracy performance.

The efficiency of the ballbar system for the calibration has been shown in the results of this study. Although the resolution of the ballbar is 0.1 μm and thus at least 100 times greater than the printer's, its application has clear benefits. The methodology applied has been validated to increase accuracy in low-cost 3D printing. Large error reductions have been achieved through error modeling with a maximum reduction of 98% in squareness error, and over 50% reductions in total circularity errors together with achieving an average radius for the ballbar within 1 μm of the programmed radius. For a system that uses low-cost, low-resolution stepper motors with a 1.9° step with a 20-tooth pulley and MXL belt-driven feed system, the system is very good compared with high-precision CNC systems with ballscrew feed systems where achieving micron accuracy is challenging. Fig. 4 shows that the high-resolution ballbar can capture vibrational effects in the printing process. The vibrations recorded on the error trace from the ballbar show that the prevalence of these vibrational effects is also reduced from the error compensation but has not been quantified in this study. As shown in this paper, microtuning of a CNC machine for high accuracy requires a rigorous and systematic approach, but the interplay between machine errors is complex and an iterative process will lead to further

developments. The approach presented here allows for rigorous tuning in a systematic and thorough manner either periodically or during the initial machine manufacturing. The ballbar method itself can be used for frequent checking of the 3D printer's accuracy, precision, and consistency during the manufacturing process and the machine lifetime.

5. Conclusion

The advancements in accuracy and precision presented in this paper are particularly important as the application of low-cost 3D printing increases and its potential is further actualized. A key aspect of this study is the application of a standardized method, ISO 230:4, for error assessment of 3D printing systems. As 3D printing advances at a dramatic rate, guidance and certification from standard-setting authorities are needed to promote and achieve high levels of manufacturing quality in 3D printing and patient-specific devices. As observed from "Process Validation and Acceptance Activities" in reference 7, careful consideration is necessary when using an additive manufacturing process for a patient-specific or batch-produced medical device. A key advantage of the ballbar and ISO 230-4 in this instance is its use of quality assurance between 3D printing systems. This approach can be used to validate the machine's CNC system, thereby ensuring quality when transferring a process developed from one 3D printer to another. Furthermore, the advancements in accuracy and contouring performance in this study are important where functional components are to be produced. With regard to the production of prosthetics, orthotics, and other patient-specific devices, these improvements in accuracy and contouring are not only key for aesthetic enhancement but are major factors in the fundamental mechanism of 3D printing, where the accuracy and precision of the layer process affects the surface roughness and interlayering bonding strength, thereby influencing mechanical and fatigue performance. As shown in standard manufacturing, higher tolerances become ever more important in the longevity and efficiency of functional components for the fine control of wear and material properties and consistency. Higher accuracies on these low-cost systems, as controlled and tested by standardized methods such as from ISO or ASTM, enables the impact and functionality of produced components to improve considerably.

Acknowledgment

This research was supported by Science Foundation Ireland through the I-Form Advanced Manufacturing Research Centre 16/RC/3872.

References

1. Berman B. 3-D printing: the new industrial revolution. Bus Horiz 2012;55(2):155-62.
2. Wulle F, Coupek D, Schäffner F, et al. Workpiece and machine design in additive manufacturing for multi-axis fused deposition modeling. Procedia CIRP 2017;60:229-34.
3. Keaveney S, Connolly P, Ahearne E, et al. Kinematic error modelling of a multi-cone frustum artefact. Machine tools technology foundation proceedings; 2014.
4. Cajal C, Santolaria J, Velazquez J, et al. Volumetric error compensation technique for 3D printers. Procedia Eng 2013;63:642-9.
5. ISO230-4. *Test code for machine tools — part 4: circular tests for numerically controlled machine tools*. 2005. [2005].
6. Xiang S, Altintas Y. Modeling and compensation of volumetric errors for five-axis machine tools. Int J Mach Tool Manuf 2016;101:65-78.
7. FDA. *Technical considerations for additive manufactured medical devices - guidance for industry and food and drug administration staff*. 2017.
8. Kersting P, Odendahl S. Capabilities of a process simulation for the analysis of five-axis milling processes in the aerospace industry. 18th International Seminar on High Technology; 2013. p. 26-47.
9. Keaveney S, Connolly P, Ahearne E, et al. Investigation of a multi-cone variant of the standard cone frustum test for 5-axis machine tools. Procedia CIRP 2014;14:317-22.
10. Masashi Y, Hamabata N, Ihara Y. Evaluation of linear axis motion error of machine tools using an R-test device. Procedia CIRP 2014;14:311-6.
11. Ibaraki S, Sawada M, Matsubara A, et al. Machining tests to identify kinematic errors on five-axis machine tools. Precis Eng 2009;34(3):387-98.
12. Bryan JB. *Telescoping magnetic ball bar test gage*. 1984.
13. Chen J, Lin S, Zhou X, et al. A ballbar test for measurement and identification the comprehensive error of tilt table. Int J Mach Tool Manuf 2016;103:1-12.
14. Liu HL, Shi HM, Li B. A new method and instrument for measuring circular motion error of NC machine tools. Int J Mach Tool Manuf 2005;45(11):1347-51.
15. Srivastava AK, Veldhuis SC, Elbestawit MA. Modelling geometric and thermal errors in a five-axis CNC machine tool. Int J Mach Tool Manuf 1995;35(9):1321-37.
16. Srewart D. A platform with six degrees of freedom. Arch Proc Inst Mech Eng 1965;180:371-86. 1847–1982 (vol. 1–196). (1965).
17. Fan JW, Guan JL, Wang WC, et al. A universal modeling method for enhancement the volumetric accuracy of CNC machine tools. J Mater Process Technol 2002;129(1–3):624-8.